NJC

LETTER

View Article Online
View Journal | View Issue

Cite this: *New J. Chem.*, 2019, 43, 2875

Received 7th November 2018,
Accepted 22nd January 2019

DOI: 10.1039/c8nj05656k

rsc.li/njc

ESIPT-based fluorescence probe for the ratiometric detection of superoxide†

Luling Wu, [a] Liyuan Liu, [a] Hai-Hao Han, [b] Xue Tian, [a] Maria L. Odyniec, [a] Lei Feng, [ac] Adam C. Sedgwick, *[d] Xiao-Peng He, [b] Steven D. Bull *[a] and Tony D. James *[a]

A simple ESIPT-based fluorescence probe (HMBT-LW) was developed for the detection of superoxide ($O_2^{\bullet-}$). HMBT-LW was synthesised over two steps and was shown to rapidly detect low concentrations of $O_2^{\bullet-}$ (limit of detection = 7.4 μM), fully reacting within two minutes. Furthermore, HMBT-LW demonstrated excellent selectivity and sensitivity towards $O_2^{\bullet-}$.

Reactive oxygen species (ROS) are the transient by-products generated from the electron transport chain.[1] More specifically, the ROS, superoxide ($O_2^{\bullet-}$) is a anion radical generated from the single electron reduction of molecular oxygen (O_2), which means $O_2^{\bullet-}$ is the precursor to most ROS.[2] $O_2^{\bullet-}$ is capable of reacting with nitric oxide (NO•), which generates the highly reactive nitrogen species peroxynitrite ($ONOO^-$), or with superoxide dismutase (SOD) to produce hydrogen peroxide (H_2O_2). Hydrogen peroxide can then be transformed into the highly reactive hydroxyl radical (•OH) and hypochlorous acid (HOCl). These reactive oxygen species are associated with a number of pathological processes, including cardiomyopathy, autism, diabetes mellitus, cancer and neurodegenerative disorders (*e.g.*, Alzheimer's disease and Parkinson's disease).[3–6] Therefore, the development of a fluorescence probe for the real-time detection of $O_2^{\bullet-}$ would further aid the understanding of $O_2^{\bullet-}$ related diseases in living organisms.

Excited-state intramolecular proton transfer (ESIPT) is widely used in the design of fluorescent probes[7] as ESIPT-based fluorescent probes display a number of favourable properties such as a large Stokes shift (~200 nm) and the ability to undergo ratiometric sensing. The ratiometric detection of a target analyte is ideal as it enables the determination of the concentration of the target analyte directly without need of calibration.[7–9]

Within our research group, we have developed several ESIPT-based fluorescent probes for the detection of biological reactive oxygen species as well as biological thiols.[10–13] Previously, we have developed a thiocarbamate functionalised methoxyhydroxybenzothiazole (**HMBT**) fluorescent probe **TCBT-OMe** for the detection of HOCl/ClO^- (Scheme 1). The addition of HOCl/ClO^- to **TCBT-OMe** resulted in the rapid hydrolysis (<10 s) of the thiocarbamate linker, leading to a ratiometric change in fluorescence intensity.[12]

Most fluorescent probes that are reported for the detection of $O_2^{\bullet-}$ utilise its nucleophilicity to achieve excellent selectivity over other ROS.[14–20] As a result of this, we believed the functionalisation of **HMBT** with the $O_2^{\bullet-}$ reactive trifluoromethanesulfonate unit would result in a ratiometric fluorescent probe for the detection of $O_2^{\bullet-}$ (Scheme 1).[21]

HMBT-LW was synthesized over two steps. The first step of the synthesis involved the addition of a 2 : 1 aq H_2O_2/aq HCl solution to 2-aminothiophenol and *o*-vanilin in EtOH, which formed **HMBT** in good yield (68%).[22–24] With **HMBT** in hand,

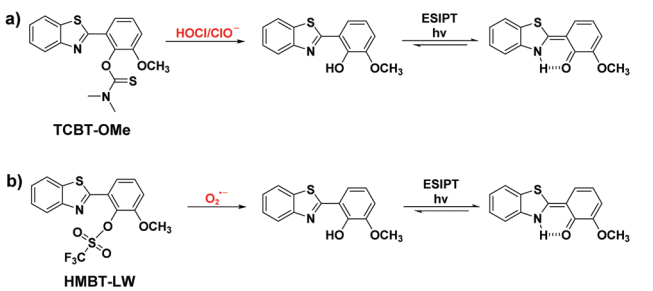

Scheme 1 (a) Our previously reported ESIPT probe for the detection of HOCl/ClO^-. (b) This work – a trifluoromethanesulfonate linker-based ESIPT **HMBT-LW** for the detection of $O_2^{\bullet-}$.

[a] Department of Chemistry, University of Bath, Bath, BA2 7AY, UK. E-mail: t.d.james@bath.ac.uk, s.d.bull@bath.ac.uk
[b] Key Laboratory for Advanced Materials and Joint International Research Laboratory of Precision Chemistry and Molecular Engineering, Feringa Nobel Prize Scientist Joint Research Center, School of Chemistry and Molecular Engineering, East China University of Science and Technology, 130 Meilong Rd., Shanghai 200237, China
[c] College of Integrative Medicine, The National & Local Joint Engineering Research Center for Drug Development of Neurodegenerative Disease, College of Pharmacy, Dalian Medical University, Dalian 116044, China
[d] Department of Chemistry, University of Texas at Austin, 105 E 24th street A5300, Austin, TX 78712-1224, USA. E-mail: a.c.sedgwick@utexas.edu

† Electronic supplementary information (ESI) available. See DOI: 10.1039/c8nj05656k

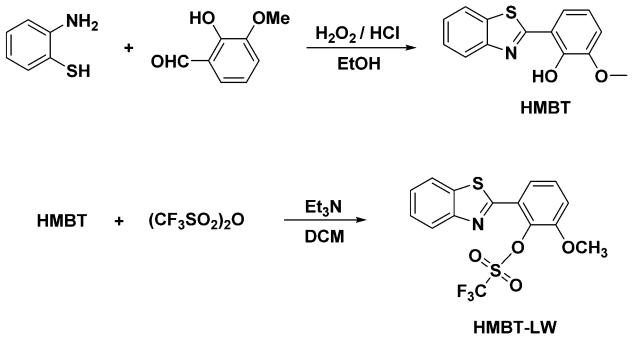

Scheme 2 Synthesis of target probe **HMBT-LW**.

trifluoromethanesulfonic anhydride was then added dropwise into a solution of **HMBT** in DCM at −78 °C under argon, NEt_3 was subsequently added to the reaction. This reaction proceeded smoothly furnishing **HMBT-LW** in good yield (52%) (Scheme 2). The chemical structure of **HMBT-LW** was fully characterized by ^1H NMR, ^{13}C NMR and high-resolution mass spectrometry (HRMS).

Next, we evaluated the UV-Vis properties of **HMBT-LW** (5 μM) with the addition of $O_2^{\bullet-}$ (42 equivalents). This addition led to an increase in UV absorption between 200–400 nm indicating a change chemical structure (Fig. S1, ESI†). We then turned our attention towards the ability of **HMBT-LW** to detect $O_2^{\bullet-}$ using fluorescence. Remarkably, **HMBT-LW** was shown to have a rapid response towards $O_2^{\bullet-}$ with a significant increase in fluorescence intensity being observed within 2 minutes (Fig. S5, ESI†). Initially, a fluorescence emission intensity at 378 nm was only observed, since the ESIPT process is blocked by the trifluoromethanesulfonate group. However, in the presence of $O_2^{\bullet-}$, a notable increase in fluorescence emission intensity at 483 nm and a simultaneously decrease in fluorescence emission intensity at 378 nm was observed (Fig. 1) corresponding to the deprotection and release of the **HMBT** fluorophore enabling the ESIPT process to take place (Reaction mechanism confirmed by HRMS – see Fig. S6 and S7, ESI†). In addition a quantum yield of 0.508 was determined for **HMBT** under these measurement conditions.[25]

HMBT-LW was then shown to have good stability over a range of different pH 4–10, (Fig. S3, ESI†) and was capable of detecting low concentrations of $O_2^{\bullet-}$ with a Limit of Detection (LoD) of 7.4 μM (Fig. S4, ESI†). Furthermore, **HMBT-LW** demonstrated excellent selectivity towards $O_2^{\bullet-}$ over other ROS and biologically relevant analytes (Fig. 2).

With this research we have developed an ESIPT-based fluorescence probe (**HMBT-LW**) for the selective and sensitive detection of $O_2^{\bullet-}$. Sadly, the excitation wavelength for **HMBT-LW** is too short to enable its use in cellular imaging experiments. However, we are currently exploring related ESIPT based systems with longer excitation wavelengths that are more suitable for cellular imaging experiments. In summary **HMBT-LW** provides a platform on which it will be possible to develop long wavelength ESIPT-based fluorescent probes for the ratiometric selective and sensitive detection of $O_2^{\bullet-}$.

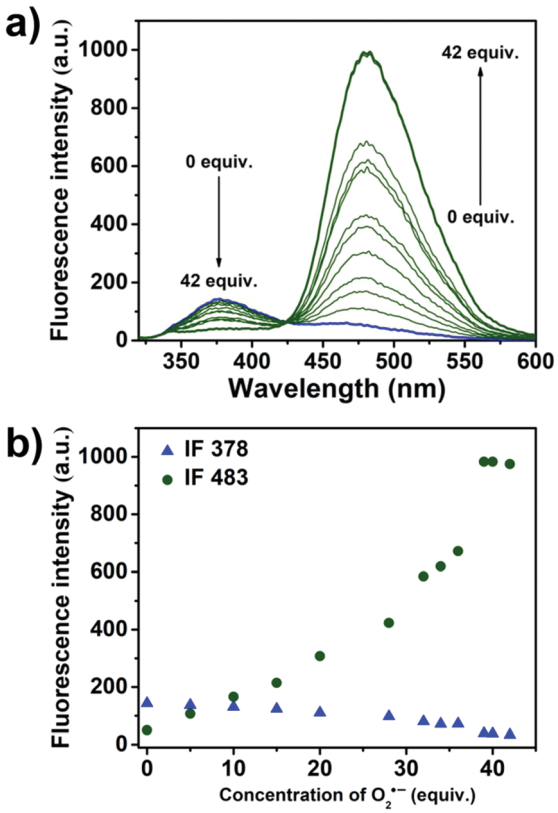

Fig. 1 (a) Changes in fluorescence emission intensity of **HMBT-LW** (5 μM) with increasing additions of $O_2^{\bullet-}$ (from 0 to 42 equiv.) in PBS buffer solution (10 mM, V/V, DMSO/PBS = 1/1, pH = 7.4) after 3 min. (b) Emission at 378 and 483 nm of **HMBT-LW** (5 μM) with increasing addition of $O_2^{\bullet-}$ (from 0 to 42 equiv.) in PBS buffer solution (10 mM, V/V, DMSO/PBS = 1/1, pH = 7.4) after 3 min. λ_{ex} = 310 nm. Slit widths: ex = 8 nm, em = 5 nm.

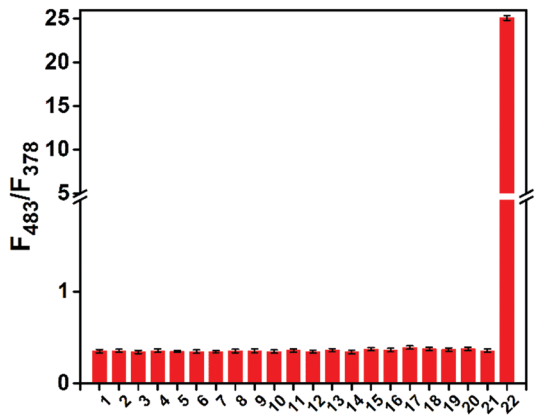

Fig. 2 Fluorescence intensity ratio changes (based on the peak heights at the maxima, 378 and 483 nm respectively) with addition of $O_2^{\bullet-}$ (39 equiv.) and other interfering reagents (120 μM). 1. Probe only; 2. ClO^-; 3. H_2O_2; 4. $^{\bullet}OH$; 5. $^1O_2$; 6. $ONOO^-$; 7. $ROO^{\bullet}$; 8. H_2S; 9. glucose; 10. GSH; 11. Cys; 12. Hcy; 13. Na^+; 14. K^+; 15. Ca^{2+}; 16. Mg^{2+}; 17. Zn^{2+}; 18. Fe^{2+}; 19. Al^{3+}; 20. Cu^{2+}; 21. Fe^{3+}; 22. $O_2^{\bullet-}$. λ_{ex} = 310 nm. Error bar represents s.d. Slit widths: ex = 8 nm, em = 5 nm. 30 min wait between measurements.

Conflicts of interest

No conflicts of interest.

Acknowledgements

LW wishes to thank China Scholarship Council and the University of Bath for supporting his PhD work in the UK. We would like to thank the EPSRC and the University of Bath for funding. TDJ wishes to thank the Royal Society for a Wolfson Research Merit Award. NMR characterisation facilities were provided through the Material and Chemical Characterisation Facility (MC^2) at the University of Bath (http://go.bath.ac.uk/mc2). The EPSRC UK National Mass Spectrometry Facility at Swansea University is thanked for analyses.

Notes and references

1 P. Held, *An Introduction to Reactive Oxygen Species – Measurement of ROS in Cells*, BioTek Instruments, 2010.
2 J. F. Turrens, *J. Physiol.*, 2003, **552**, 335–344.
3 S. Rose, S. Melnyk, O. Pavliv, S. Bai, T. G. Nick, R. E. Frye and S. J. James, *Transl. Psychiatry*, 2012, **2**, e134.
4 R. A. Cairns, I. S. Harris and T. W. Mak, *Nat. Rev. Cancer*, 2011, **11**, 85–95.
5 C. Gorrini, I. S. Harris and T. W. Mak, *Nat. Rev. Drug Discovery*, 2013, **12**, 931–947.
6 M. H. Lee, J. S. Kim and J. L. Sessler, *Chem. Soc. Rev.*, 2015, **44**, 4185–4191.
7 A. C. Sedgwick, L. Wu, H.-H. Han, S. D. Bull, X.-P. He, T. D. James, J. L. Sessler, B. Z. Tang, H. Tian and J. Yoon, *Chem. Soc. Rev.*, 2018, **47**, 8842–8880.
8 Y.-W. Wang, Y.-X. Hua, H.-H. Wu, X. Sun and Y. Peng, *Chin. Chem. Lett.*, 2017, **28**, 1994–1996.
9 Z.-H. Fu, X. Han, Y. Shao, J. Fang, Z.-H. Zhang, Y.-W. Wang and Y. Peng, *Anal. Chem.*, 2017, **89**, 1937–1944.
10 L. Wu, H.-H. Han, L. Liu, J. E. Gardiner, A. C. Sedgwick, C. Huang, S. D. Bull, X.-P. He and T. D. James, *Chem. Commun.*, 2018, **54**, 11336–11339.
11 L. Wu, Y. Wang, M. Weber, L. Liu, A. C. Sedgwick, S. D. Bull, C. Huang and T. D. James, *Chem. Commun.*, 2018, **54**, 9953–9956.
12 L. Wu, Q. Yang, L. Liu, A. C. Sedgwick, A. J. Cresswell, S. D. Bull, C. Huang and T. D. James, *Chem. Commun.*, 2018, **54**, 8522–8525.
13 A. C. Sedgwick, X. Sun, G. Kim, J. Yoon, S. D. Bull and T. D. James, *Chem. Commun.*, 2016, **52**, 12350–12352.
14 P. Li, W. Zhang, K. Li, X. Liu, H. Xiao, W. Zhang and B. Tang, *Anal. Chem.*, 2013, **85**, 9877–9881.
15 X. Han, R. Wang, X. Song, F. Yu, C. Lv and L. Chen, *Biomaterials*, 2018, **156**, 134–146.
16 Y. Lv, D. Cheng, D. Su, M. Chen, B.-C. Yin, L. Yuan and X.-B. Zhang, *Chem. Sci.*, 2018, **9**, 7606–7613.
17 J. J. Hu, N.-K. Wong, S. Ye, X. Chen, M.-Y. Lu, A. Q. Zhao, Y. Guo, A. C.-H. Ma, A. Y.-H. Leung, J. Shen and D. Yang, *J. Am. Chem. Soc.*, 2015, **137**, 6837–6843.
18 D. P. Murale, H. Kim, W. S. Choi and D. G. Churchill, *Org. Lett.*, 2013, **15**, 3946–3949.
19 D. Lu, L. Zhou, R. Wang, X.-B. Zhang, L. He, J. Zhang, X. Hu and W. Tan, *Sens. Actuators, B*, 2017, **250**, 259–266.
20 Z. Zhang, J. Fan, Y. Zhao, Y. Kang, J. Du and X. Peng, *ACS Sens.*, 2018, **3**, 735–741.
21 A. Sytnik and M. Kasha, *Proc. Natl. Acad. Sci. U. S. A.*, 1994, **91**, 8627–8630.
22 X. Yang, Y. Guo and R. M. Strongin, *Angew. Chem., Int. Ed.*, 2011, **50**, 10690–10693.
23 J. Dey and S. K. Dogra, *J. Photochem. Photobiol., A*, 1992, **66**, 15–31.
24 G. F. Kirkbright, D. E. M. Spillane, K. Anthony, R. G. Brown, J. D. Hepworth, K. W. Hodgson and M. A. West, *Anal. Chem.*, 1984, **56**, 1644–1647.
25 H. Li, Q. Yao, J. Fan, J. Du, J. Wang and X. Peng, *Biosens. Bioelectron.*, 2017, **94**, 536–543.